

Neutron thermodiffraction study of the crystallization of Ag–Ge–Se glasses: evidence of a new phase

This article has been downloaded from IOPscience. Please scroll down to see the full text article.

2008 J. Phys.: Condens. Matter 20 155106

(<http://iopscience.iop.org/0953-8984/20/15/155106>)

View [the table of contents for this issue](#), or go to the [journal homepage](#) for more

Download details:

IP Address: 129.252.86.83

The article was downloaded on 29/05/2010 at 11:28

Please note that [terms and conditions apply](#).

Neutron thermodiffraction study of the crystallization of Ag–Ge–Se glasses: evidence of a new phase

Andrea A Piarristeguy¹, Gabriel J Cuello², Pascal G Yot¹,
Michel Ribes¹ and Annie Pradel¹

¹ Institut Charles Gerhardt, Equipe PMDP UMR 5253 CNRS, CC1503,
Université Montpellier 2, F-34095 Montpellier Cedex 5, France

² Institut Laue Langevin, 6 rue Jules Horowitz, BP 156, F-38042 Grenoble Cedex 9, France

E-mail: andrea.piarristeguy@lpmc.univ-montp2.fr, cuello@ill.eu, pyot@lpmc.univ-montp2.fr,
mribes@lpmc.univ-montp2.fr and apradel@lpmc.univ-montp2.fr

Received 14 December 2007, in final form 31 January 2008

Published 10 March 2008

Online at stacks.iop.org/JPhysCM/20/155106

Abstract

Silver-containing chalcogenide glasses are potential candidates for electrical memory manufacturing. In order to study the glasses under dynamic conditions, using the temperature as the main parameter, a neutron thermodiffraction study of three $\text{Ag}_x(\text{Ge}_{0.25}\text{Se}_{0.75})_{100-x}$ glasses ($x = 5, 15$ and 25) was carried out. Two *in situ* diffraction experiments were performed: a first series including heating ramps from room temperature up to 350°C and a second one comprising the measurement of an isotherm at about 300°C for 5 h. For the three studied glasses two stable crystalline phases were formed during the heating process: the cubic Ag_8GeSe_6 appeared first, followed by the crystallization of monoclinic GeSe_2 . The crystallization process for the Ag-rich ($x = 15$ and 25) glasses was more complex, with the appearance of a new unstable phase at high temperature, i.e. Ag_2GeSe_3 . Such a phase decomposed with time or temperature to produce a new phase, $\text{Ag}_{10}\text{Ge}_3\text{Se}_{11}$, along with the stable GeSe_2 . This phase has never been reported to date while the existence of Ag_2GeSe_3 was still controversial.

(Some figures in this article are in colour only in the electronic version)

1. Introduction

For many years chalcogenide glasses have been widely investigated since several of their properties make them very attractive materials. They possess a large ionic conductivity—two to three orders of magnitude larger than that of the oxide glasses with the same mobile ion content. For example, Ag–Ge–Se glasses evolve from semiconductors to superionic conductors when the Ag concentration is increased ($\sigma = 10^{-4} \Omega^{-1} \text{cm}^{-1}$ for $\text{Ag}_{25}\text{Ge}_{18.75}\text{Se}_{56.25}$ glass at room temperature) [1–9]. Moreover thin layers of chalcogenide glasses, deposited by thermal evaporation or RF sputtering, exhibit photoinduced phenomena which are at the basis of many interesting applications [10]. In particular, Ag photodissolution or photodeposition in a chalcogenide layer can be used to produce diffraction gratings, microlenses or

optical memory. More recently, a new type of electrical memory based upon the high mobility of silver in chalcogenide glasses has been proposed [11]. A programmable metallization cell—PMC—memory typically comprises a silver-photodoped glassy thin film of composition $\approx \text{Ge}_{0.25}\text{Se}_{0.75}$ placed between two electrodes, a silver one and a nickel one for example. The conductivity of the film is reversibly changed by several orders of magnitude when a weak voltage is applied (≈ 0.3 V). When applied to nanometric devices (when the thickness of the glassy film is typically 20–30 nm), the phenomenon is characterized by a very short time for commutation (≈ 10 ns) and a very high cyclability ($> 10^6$ cycles). The assumption that a phase separation with the presence of silver rich domains would exist in the film was proposed to explain the phenomenon [11]. However, no clear understanding of the phenomenon is known to date.

At a first stage, our investigation is focused on bulk glasses of the Ag–Ge–Se system. A series of experiments was recently carried out on $\text{Ag}_x(\text{Ge}_{0.25}\text{Se}_{0.75})_{100-x}$ glasses with $1 < x < 30$ at.%. The combined investigation of electrical conductivity by complex impedance spectroscopy and microstructure by field emission scanning electron microscopy and/or electric force microscopy (that give information on the presence of chemical contrasts and electrical inhomogeneity, respectively) helped in understanding the difference of seven to eight orders of magnitude in the conductivity of the system: the glasses were phase separated and the percolation of the Ag-rich phase was at the origin of a sudden jump in conductivity [12, 13]. The structure of the $\text{Ag}_x(\text{Ge}_{0.25}\text{Se}_{0.75})_{100-x}$ glasses with $x = 5, 15$ and 25 at.% (hereafter named Ag5, Ag15 and Ag25, respectively) was then studied by neutron diffraction and *ab initio* molecular dynamic simulations at different temperatures. The presence of both Se–Se and Ge–Se correlations in the first peak of the radial distribution function was consistent with a structure containing both $\text{GeSe}_{4/2}$ tetrahedra and Se–Se bonds [14]. According to the simulation results, the silver environment depends very much on the silver content in the glassy matrix. While the glass with the lowest silver content (Ag5) presented only one correlation peak at 4.4 \AA , the Ag-rich glasses presented two peaks: a main peak at 3 \AA and a less intense peak at 4.4 \AA . This result could be related to the electrical properties of the materials, namely a very low conductivity for the Ag5 sample and a fast Ag^+ conductivity for the samples Ag15 and Ag25 [15].

At this point, only static measurements were performed to investigate the Ag–Ge–Se glasses. However, the functioning of a PMC device implies a dynamic process with an applied voltage on a miniaturized component and therefore some energy transfer to the glassy Ag–Ge–Se film. Therefore, a complementary investigation of the bulk glasses under dynamic conditions was thought pertinent to bring additional information to understand the phenomena underlying the functioning of PMC. At this point the temperature was chosen as the parameter to study the glasses under dynamic conditions, and, more precisely, an *in situ* neutron thermodiffraction investigation of glasses from the Ag–Ge–Se system was considered.

In the paper we report on the results of the investigation, i.e. on the crystallization process of the $\text{Ag}_x(\text{Ge}_{0.25}\text{Se}_{0.75})_{100-x}$ glasses with $x = 5, 15$ and 25 at.% using the *in situ* neutron thermodiffraction technique. As expected from the Ag–Ge–Se phase diagram, two stable crystalline phases, Ag_8GeSe_6 and GeSe_2 , were formed during the heating process; more unexpected was the appearance of additional high temperature phases in the Ag-rich glasses [16]. The characterization of these new phases, in particular their temperature and time dependence and their dependence on silver content, are discussed in the paper.

2. Experimental details

Three compositions of bulk glasses (Ag5, Ag15 and Ag25) were prepared from high-purity (4N) elements by the melt-quenching technique. The materials were synthesized by

placing the powdered elements in stoichiometric proportions in a cylindrical quartz ampoule. The batches were evacuated to a pressure of $\approx 10^{-5}$ mbar and sealed. After synthesis and homogenization for 7 h at $T = 1200 \text{ K}$ in a furnace, the ampoules were quenched in a mixture of ice and water to obtain the glassy materials.

The neutron thermodiffraction technique was used to study the crystallization of the glasses upon heating and in isothermal conditions. The neutron diffraction experiments were performed using the D1B instrument at the Institut Laue–Langevin (Grenoble, France). The instrument is a two-axis diffractometer having a banana-like ^3He wire detector with 400 cells placed in a cylindrical geometry centred at the sample position. Such a detector, combined with the high neutron flux ($\approx 6 \times 10^6 \text{ n s}^{-1} \text{ cm}^{-2}$), allowed the collection of a complete 80° -diffractogram (with steps of 0.2°) in about 5 min (for the heating ramps) and 15 min (in the isothermal conditions).

The containers with the samples were placed inside a 0.2 mm thick vanadium wrap, which was located in a standard ILL furnace (vertical top loading furnace). The heating element was a vanadium cylinder with a diameter of 30 mm and a 0.1 mm thick wall, which was in the centre of an evacuated aluminium chamber. The incident neutron wavelength (2.52 \AA nominal) was selected by using a pyrolytic graphite monochromator (plane 002). The exact values of the wavelength and the zero-angle correction were determined by means of an independent measurement using an Al_2O_3 powder sample as a standard.

Two sets of diffraction experiments were performed: the first one while the sample was heated up to 350°C and the second one in isothermal conditions at about 300°C .

2.1. Heating ramps

The samples were placed in sealed cylindrical quartz containers of 12 mm outer diameter and 10 mm inner diameter. These diameters were chosen in order to get an optimal signal to noise ratio. The containers were wrapped in 0.1 mm thick vanadium foil and hung at the geometrical centre of the detector. The furnace and its control system allowed performing ramps at a heating rate of $0.2^\circ\text{C min}^{-1}$, from room temperature up to 350°C , while neutron diffraction spectra were continuously registered. Each diffraction pattern is the result of the accumulation of the spectra recorded over 5 min, i.e. during an increase in temperature of 1°C . For the cooling process, the furnace was switched off and the samples were allowed to reach room temperature in ‘free fall’.

The spectrum for the alumina standard allowed calibrating the incident neutron wavelength and zero-angle correction, i.e. $2.5295(1) \text{ \AA}$ and $0.1834(2)^\circ$, respectively.

2.2. Isotherm at 298°C

The samples were placed in non-sealed cylindrical vanadium containers with an outer diameter of 8 mm and an inner diameter of 7.6 mm , in vacuum. The samples were heated from room temperature to 200°C at a rate of $10^\circ\text{C min}^{-1}$, and then between 200°C and 298°C at $0.2^\circ\text{C min}^{-1}$. The samples were kept at this temperature for 5 h while diffraction patterns were

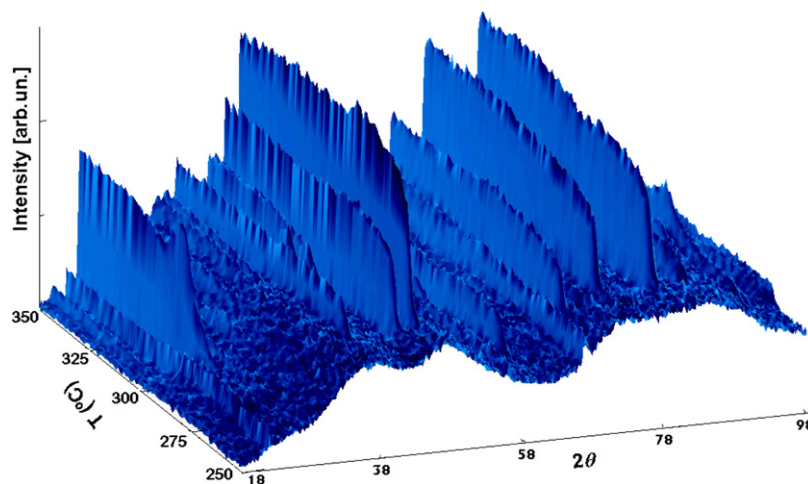


Figure 1. Neutron thermodiffractogram for the Ag25 sample during the heating ramp from 250 °C up to 350 °C.

recorded every 15 min. The samples were then cooled down as explained in the previous subsection. The same calibration procedure was applied to find 2.5276(9) Å for the incident neutron wavelength and 0.20(3)° for the zero-angle correction.

3. Results

3.1. Heating ramps

3.1.1. Crystallization of stable phases. Figure 1 shows a 3D plot of the recorded diffraction patterns for the Ag25 glass between 250 and 350 °C. Similar 3D plots were obtained for the Ag5 and Ag15 glasses. The diffraction halos observed in the background were expected and at least partially due to the presence of the quartz container. However, a contribution of the chalcogenide glass cannot be discarded even at the highest temperatures. The appearance of several sets of peaks at different temperatures is the signature of the glass crystallization during the heating process. Owing the temperatures of measurements much larger than that of the glass transition at about 230 °C, such a crystallization was expected.

The diffraction patterns were analysed using the Rietveld method, i.e. minimizing the quadratic difference between the calculated and measured spectra and varying parameters such as the fraction of present phases, lattice constants, occupation of atomic sites, and Debye–Waller factors, among other instrumental parameters [17]. The peak-shape function used is the pseudo-Voigt function. Such an analysis was rather difficult because of the presence of the amorphous background due to the quartz container. However, it was not too crucial because the objective was the study of the glass crystallization and not the refinement of the structure.

In a first analysis, it appeared clearly that two main phases crystallized in the three samples during the heating process: the cubic form of the Ag₈GeSe₆ phase appeared first, followed by the GeSe₂ phase. These were the expected phases according to the phase diagram of the Ag–Ge–Se system that was proposed by Prince [18]. For the Ag25 sample, the crystallization temperature of the Ag₈GeSe₆ phase was 266.5(3) °C and

the peak intensity increased drastically at once (the maximal intensity was recovered in less than 1 °C). Approximately 30 °C later, the GeSe₂ phase started crystallizing, as can be seen in figure 1. A similar behaviour was observed for the Ag15 sample, but the crystallization of the Ag₈GeSe₆ phase was slower (the maximal intensity for the main peak was recovered after an increase in temperature of more than 3 °C) and occurred later on at 270.6(5) °C. The crystallization of GeSe₂ occurred at 287 °C. As for the Ag5 sample, the diffraction peaks of the two crystalline phases appeared almost simultaneously at 280 °C and 288 °C, respectively. It was not surprising to find that the contribution of the GeSe₂ phase was larger for the sample with the smallest amount of silver (Ag5). On the whole, the appearance of the argyrodite phase occurs at a temperature that decreases as the silver content of the glass increases, while the phase GeSe₂ appears at a higher temperature for the silver rich glass.

3.1.2. Appearance of an additional phase

Temperature dependence. Now let us consider more closely the diffraction patterns of sample Ag25; we focus on different regions of the spectra for temperatures comprised between 285 and 324 °C, shown in figure 2. While most of the peaks are the signature of the two crystalline phases Ag₈GeSe₆ and GeSe₂, additional peaks are observed. For example, the peak at about $2\theta = 39^\circ$ belongs neither to the argyrodite nor to the GeSe₂ phase. It is the signature of a third unknown phase, that begins to crystallize at about 285 °C.

The interplanar distances d_{hkl} and the relative intensities I of the peaks that were to be attributed to the third phase are given in table 1. The three main peaks appeared at 2θ values of 24.2°, 50.2° and 39°, with their relative intensities being 100%, 86% and 43%, respectively. The intensity of the peaks kept increasing from 285 °C, when the peaks first appeared, up to approximately 300 °C, and then started decreasing strongly.

Above 315 °C two different behaviours were observed. Examples of both of them are given in figure 3 for the

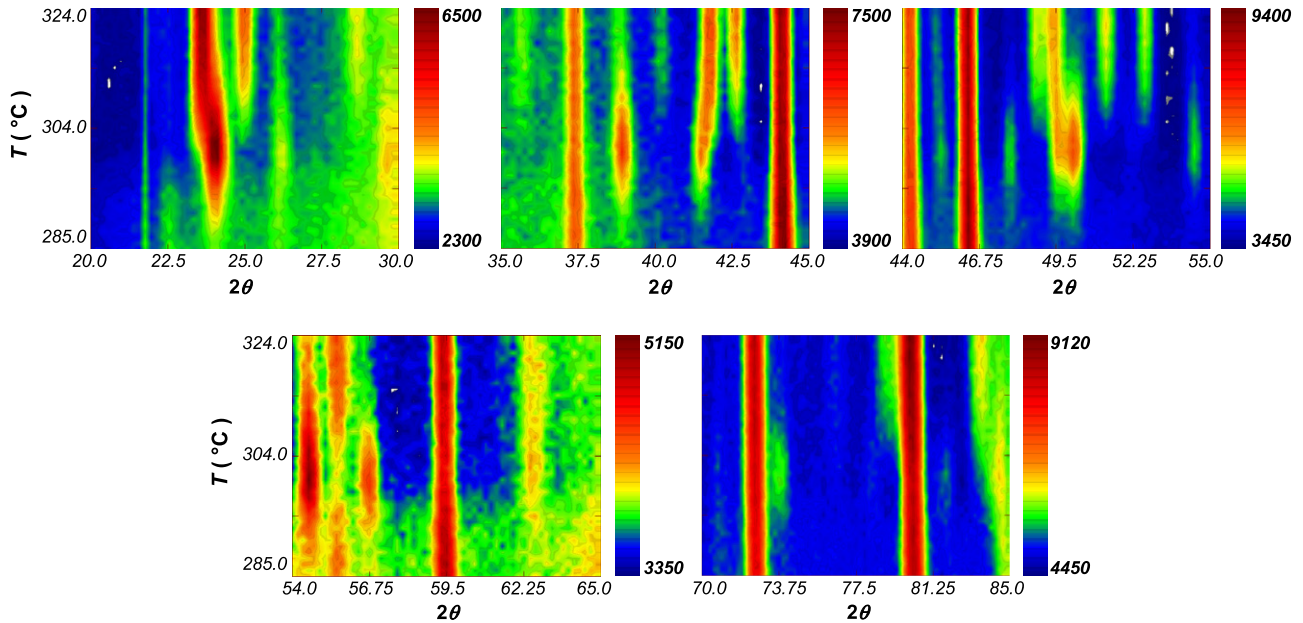


Figure 2. Neutron thermodiffractograms for the Ag25 sample during the heating ramp from 285 °C up to 324 °C ($\lambda = 2.5295(1) \text{ \AA}$). These images reveal clearly the presence of a ‘third’ phase.

Table 1. Interplanar distances d_{hkl} and relative intensities I of the peaks of the ‘third’ phase for the Ag25 sample during the heating process and the isotherm at 298 °C. The entries labelled with * correspond to those peaks that do not disappear during the heating ramps, and they are still present in the cooling process.

d_{hkl}	Heating ramps		Isotherm at 298 °C		
	2θ	I (%)	d_{hkl}	2θ	I (%)
6.03	24.2	100	5.93	24.6	100
4.92	29.8	12.9	4.82	30.4	12.6
3.79	39.0	43.5*	3.73	39.6	34.8*
3.56	41.6	41.9	3.51	42.2	33.6
3.11	48.0	25.9	3.08	48.4	18.1
2.98	50.2	86.4	2.96	50.6	61.2
2.76	54.6	37.5*	2.74	55.0	28.3*
2.66	56.8	23.2	2.63	57.4	15.4
2.11	73.8	24.0	2.10	74.2	19.4
1.93	82.0	10.7	1.92	82.2	10.3

peaks at $2\theta = 50.2^\circ$ and 39° . In the first case the peak completely disappeared above 315 °C, while in the second case the decrease in the peak intensity stopped at this temperature and the intensity remained unchanged afterwards. Two peaks only are concerned by this behaviour, i.e. the peaks at $2\theta = 39^\circ$ and 54.6° .

In addition, it is clear from figures 2 and 3 that (a) the appearance of the third phase had no impact on the crystalline phase Ag_8GeSe_6 (no change in the intensity of the peaks for example) and (b) the temperature at which the third phase started disappearing (as attested by the decrease in the peak intensity) matched the temperature of crystallization of GeSe_2 .

Another point to be noted is the fact that the two peaks of the third phase, that did not disappear during the heating ramps, were still present in the spectra recorded during the cooling process and at room temperature.

Silver content dependence. 2D images of the neutron thermodiffractograms of the three samples Ag25, Ag15 and Ag5 in the interval $2\theta = 20^\circ\text{--}30^\circ$ are shown in figure 4. While the signature of the third phase is still present for sample Ag15 it is absent for sample Ag5. Figure 5 shows the evolution of the main peak of the third phase with the temperature for both samples Ag15 and Ag25. The temperature domain where the third phase was observed is slightly narrower for sample Ag15 than for sample Ag25 ($285^\circ\text{--}320^\circ\text{C}$ for Ag25 and $276^\circ\text{--}296^\circ\text{C}$ for Ag15) and displaced 20°C towards a lower temperature.

Not all the peaks present in Ag25 were found in Ag15, and the intensity of the observed ones was reduced by $\approx 33\text{--}54\%$. Therefore, the contribution of the third phase is clearly less important in Ag15 than in Ag25.

3.2. Isotherm at 298 °C

The annealing process at $T = 298^\circ\text{C}$ helped in investigating the kinetics of crystallization of sample Ag25. Figure 6 shows the neutron diffractograms of sample Ag25 at 298 °C for six different annealing times (15 min, 1, 2, 3, 4 and 5 h). Focuses on different regions of the spectrum recorded after an annealing of 5 h are shown in figure 7. The changes in the relative intensities of the peaks, indicative of the growth of some phases, are clearly evidenced.

The cubic Ag_8GeSe_6 phase was present from the beginning of the annealing process and no change in the intensity of the peak was observed throughout the whole process. The contribution of the phase GeSe_2 was appreciable after 1 h of annealing. The third phase was also observed. The same reflections as those observed in the spectra recorded during the heating process were indeed present, even though the relative intensities of the peaks given in table 1 are not exactly the same. The intensity of the peaks depended on

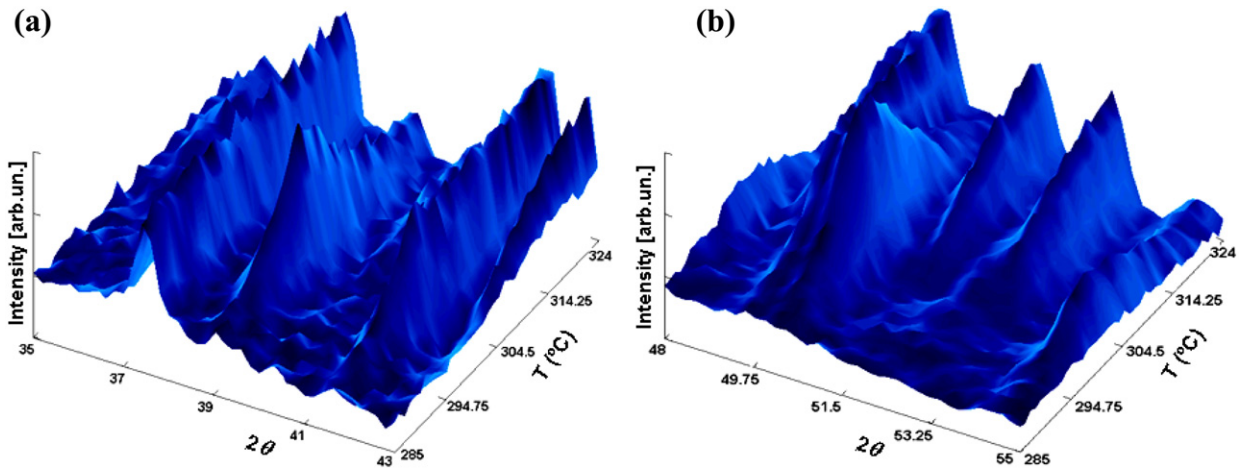


Figure 3. Neutron thermodiffractogram for the Ag25 sample during the heating ramp from 285 °C up to 324 °C. The graphs show specifically the peaks (a) $2\theta = 39^\circ$, whose intensity started decreasing above 320 °C and finally remained constant for the remaining part of the heating process, and (b) $2\theta = 50.2^\circ$, that started decreasing in intensity at 300 °C to disappear completely at about 315 °C.

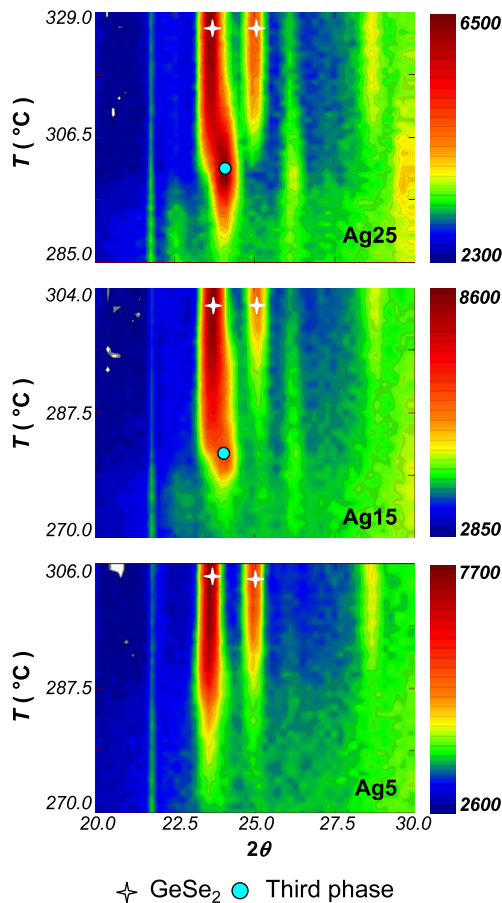


Figure 4. Neutron thermodiffractogram for the $\text{Ag}_x(\text{Ge}_{0.25}\text{Se}_{0.75})_{100-x}$ system with $x = 25, 15$ and 5 at.% during the heating ramp for the interval $2\theta = 20^\circ\text{--}30^\circ$.

the annealing time, suggesting the possibility of a kinetic behaviour. An increase in the intensity of the peaks was observed during the first 2 h of annealing and later diminished until the end of the heat treatment (look at the peak at $2\theta \approx 39^\circ$ in figure 6 for example).

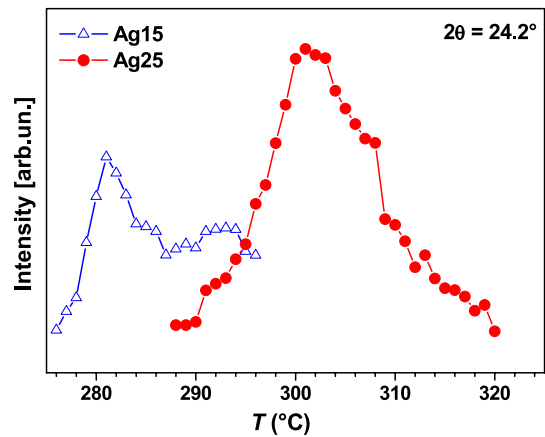


Figure 5. Temperature dependence of the main peak intensity of the ‘third’ phase for the samples Ag15 and Ag25.

4. Discussion

The stable phases that appeared during the crystallization process of the $\text{Ag}_x(\text{Ge}_{0.25}\text{Se}_{0.75})_{100-x}$ system with $x = 25, 15$ and 5 at.% are those that were expected from the phase diagram of the Ag–Ge–Se system [18], i.e. Ag_8GeSe_6 and GeSe_2 . At room temperature, the stable crystalline form for Ag_8GeSe_6 is the orthorhombic one, β' - Ag_8GeSe_6 . It changes to an FCC form, γ - Ag_8GeSe_6 , at 48 °C [19]. Therefore, it was not surprising that the Ag_8GeSe_6 phase appeared in its cubic form when it crystallized from the glass at $T \approx 266\text{--}280^\circ\text{C}$. The crystallization of the monoclinic GeSe_2 phase occurred at a higher temperature comprised between 287 and 302 °C depending on the silver content in the glass. In the meantime, at $T \approx 280\text{--}290^\circ\text{C}$, it was shown that a third phase crystallized in the two silver rich glasses Ag15 and Ag25.

Between 298 and 308 °C (for the Ag25 sample) and 280 and 290 °C (for the Ag15 sample) the peaks corresponding to the third phase either disappeared or decreased in intensity. As mentioned in section 3.1.2, such temperature domains

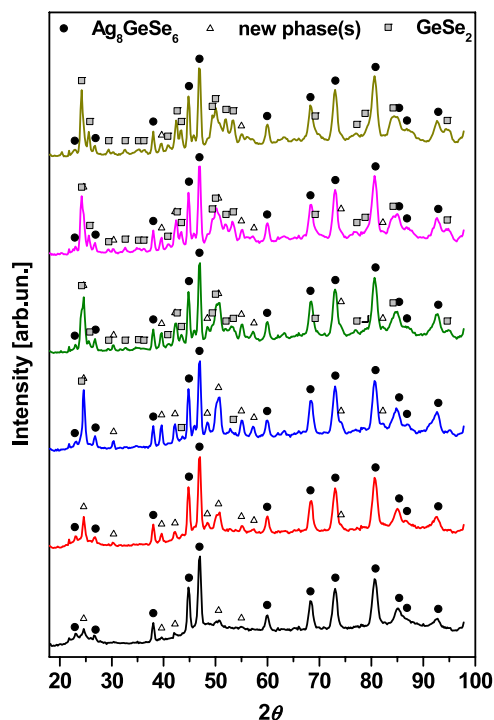


Figure 6. Neutron diffractograms for the Ag25 sample at 298 °C for six different annealing times.

matched nicely the temperature domain when GeSe₂ started crystallizing.

As shown in section 3.2, the presence of a third phase during the crystallization of glass Ag25 was confirmed by studying the change in the thermodiffraction spectra during an annealing of the glass for 5 h at 298 °C. Again additional peaks aside from those of the two stable phases were observed.

Good agreement between the positions of the additional reflections found in both experiments (heating ramps and 298 °C isotherms) confirmed the presence of the same phase in both crystallization processes. As in the case of the heating process, the peaks corresponding to the third phase started decreasing in intensity after some time to eventually disappear completely for most of them. Clearly, the ‘lifetime’ of the third phase was only a few hours, regardless of the heating treatment. Bearing in mind that every degree in the set of diffractograms corresponds to 5 min, the phase lasted for about 2 h 40 min during the heating ramps. During the isothermal treatment, this time can be extended to 5 h. However, it should be noted that two peaks (39° and 54.6°) did not disappear, the same that were present during the cooling process in the first series of experiments.

All the previous results point toward the crystallization of an unstable phase that decomposes after some time to give GeSe₂ and a fourth phase as attested by the presence of the two additional peaks that do not disappear upon heating, cooling or annealing. The additional phases are not present in the silver poor glass, whereas in the silver rich glasses the larger the Ag content, the stronger the contribution of the phases.

In 2003, Ureña *et al* [5] reported data obtained on several Ag_x(Ge_{0.25}Se_{0.75})_{100-x} glasses by differential scanning calorimetry (DSC). A similar calorimetric behaviour, i.e. a glass transition and two exothermic peaks, was observed for samples with $x = 10, 15$ and 20 at.% Ag. On the other hand, the sample with $x = 25$ at.% Ag behaved differently with a different shape in the glass transition shift, and a small exothermic peak between the two main peaks corresponding to the crystallization of Ag₈GeSe₆ and GeSe₂. The additional peak that appeared at ≈ 340 °C could be evidence of the crystallization of the third phase observed by neutron thermodiffraction. The displacement of the

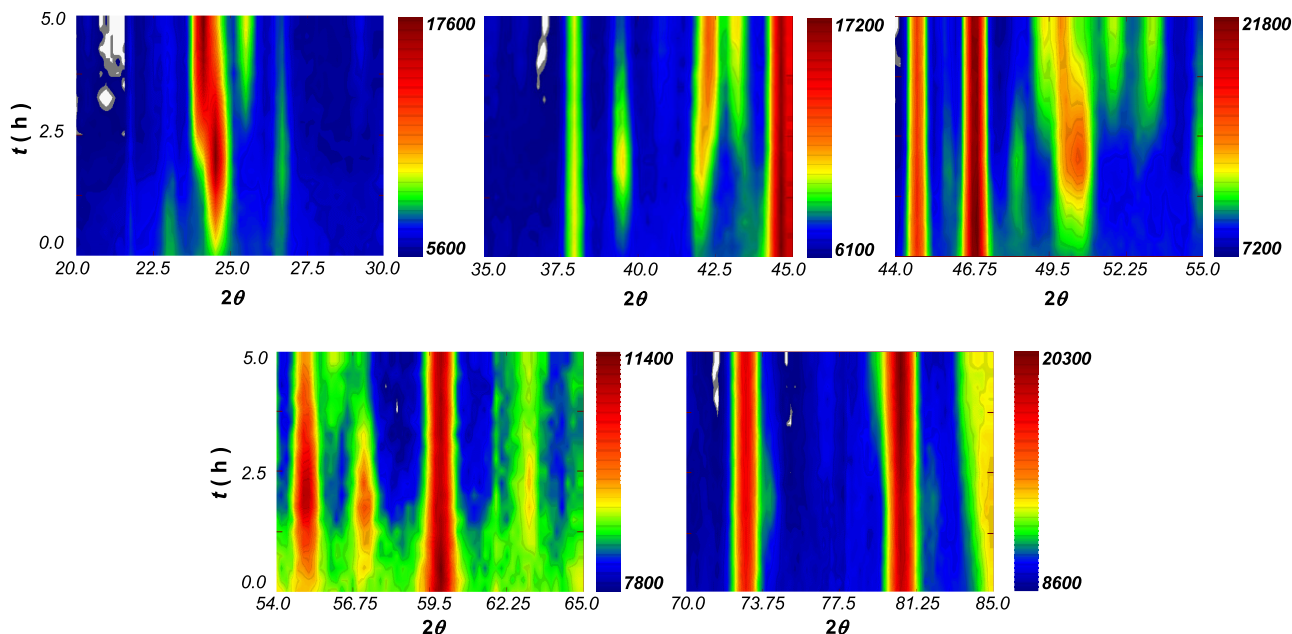


Figure 7. Neutron thermodiffraction for the Ag25 sample during the annealing at 298 °C for 5 h ($\lambda = 2.5276(9)$ Å). These images clearly reveal the presence of a ‘third’ phase.

signature at higher temperature can be explained by the different rates of the heating ramps ($10\text{ }^\circ\text{C min}^{-1}$ for DSC against $0.2\text{ }^\circ\text{C min}^{-1}$ for neutron thermodiffraction). When the heating ramps are faster, the transformations are shifted to higher temperatures, showing the thermally activated nature of the process.

Several assumptions can be made on what is the composition, structure, stability of the third and fourth phases. The third phase could be the ternary phase Ag_2GeSe_3 . No agreement exists on whether this phase exists or not. Several papers claim to prove its existence while others claim the opposite. Ollitrault-Fichet *et al* [20], Movsum-Zade *et al* [21] and Prince [18] re-constructed the phase diagram of the $\text{Ag}_2\text{Se-GeSe}_2$ system. The presence of the crystalline compound Ag_8GeSe_6 was confirmed, but the compound Ag_2GeSe_3 was not found. Movsum-Zade *et al* [21] proposed that the compound Ag_2GeSe_3 was formed by a peritectic reaction ($L_1 + \text{Ag}_8\text{GeSe}_6 \rightleftharpoons \text{Ag}_2\text{GeSe}_3$) close in temperature and composition to the eutectic point. The proximity to the eutectic would be the reason why the phase is difficult to observe. On the other hand, Prince [18] and Ollitrault-Fichet *et al* [20] observed neither the reaction nor the compound; they concluded that no other ternary crystalline phase than the Ag_8GeSe_6 one existed in the Ag-Ge-Se diagram.

Similar controversies exist on the basis of structural studies by x-ray diffraction. Velázquez-Velázquez *et al* [22] studied the compound Ag_2GeSe_3 and could index the reflections of a monoclinic phase. On the other hand, Mikolaichuk *et al* [23] studied compounds of composition $(\text{Ag}_8\text{GeSe}_6)_x(\text{GeSe}_2)_{100-x}$ with $x = 0, 25$ and 100 at.%, but only the crystalline phases Ag_8GeSe_6 and GeSe_2 were observed.

The comparison with an analogous ternary chalcogenide glass system Ag-Ge-S could help in the interpretation of the data. A structural study of the pseudo-binary system $\text{Ag}_2\text{S-GeSe}_2$ above $250\text{ }^\circ\text{C}$ revealed the existence of three ternary crystalline phases [24]. In addition to the well known Ag_8GeSe_6 phase, two other phases, i.e. Ag_2GeSe_3 and $\text{Ag}_{10}\text{Ge}_3\text{S}_{11}$, were found at high temperature.

The crystalline phase Ag_2GeSe_3 was synthesized from $\text{Ag}_2\text{S:GeSe}_2$ ratio 1:1. The reaction between the binary constituents started at about $500\text{ }^\circ\text{C}$. The phase could be obtained. However, a significant quantity can only be obtained if the solid-state reaction is carried out at $600\text{--}650\text{ }^\circ\text{C}$ and interrupted after 3 days. These samples with stoichiometric composition Ag_2GeSe_3 yielded as impurity a small amount of the dark coloured phase $\text{Ag}_{10}\text{Ge}_3\text{S}_{11}$. Both longer reaction times and higher reaction temperatures cause the decomposition of the Ag_2GeSe_3 initially produced; but once it has been produced Ag_2GeSe_3 could be stored undecomposed for months. At temperatures above $650\text{ }^\circ\text{C}$, the phase was said to decompose rapidly. The decomposition into Ag_2S and Ag_8GeSe_6 can also be observed after a very long annealing at $300\text{ }^\circ\text{C}$, which is an indication that Ag_2GeSe_3 is only metastable, at least in the preparation conditions reported in the paper. It only represents an intermediate stage in the production of Ag_8GeSe_6 from Ag_2S and GeSe_2 [25]. An orthorhombic elementary cell with $a = 11.791(5)\text{ \AA}$, $b =$

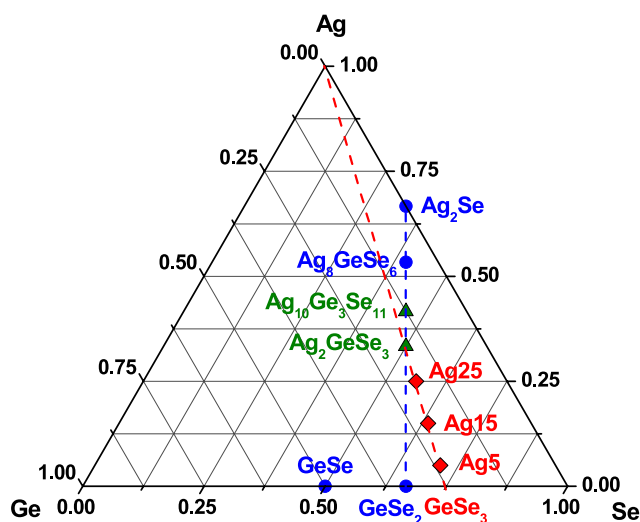


Figure 8. Composition diagram of the Ag-Ge-Se system: circles, stable crystalline phases; triangles, non-stable crystalline phases; diamonds, studied samples.

$7.079(3)\text{ \AA}$ and $c = 6.344(3)\text{ \AA}$ parameters was indexed for the powder data. Elementary cell dimensions and the intensity dependence of the main reflection allowed surmising that Ag_2GeSe_3 crystallizes in a superlattice of the wurtzite structure. Based on the observed extinction rules, hkl only present with $h + k = 2n$ and $h0l$ only present with $l = 2n$, the possible space groups were $Cmcm$, $Cmc21$ and $C2cm$ [24, 25].

The synthesis of $\text{Ag}_{10}\text{Ge}_3\text{S}_{11}$ from the elements through a stepwise addition of sulfur was similar to that described for Ag_2GeSe_3 . Homogeneity was obtained with stoichiometric composition $\text{Ag}_{10}\text{Ge}_3\text{S}_{11}$ in less than 4 days at $600\text{ }^\circ\text{C}$. Crystals of suitable size, obtained at $600\text{ }^\circ\text{C}$, differed from that of Ag_8GeSe_6 by the presence of prismatic faces parallel to the cylinder axis. With this axis as the b direction, a monoclinic unit cell was chosen with refined parameters $a = 26.206\text{ \AA}$, $b = 6.481\text{ \AA}$, $c = 25.043\text{ \AA}$ and $\beta = 109^\circ57'$. The systematic extinctions hkl ($h + k = 2n$), $h0l$ ($l = 2n$, $h = 2n$) and $0k0$ ($k = 2n$) correspond to space groups Cc or $C2/c$ [24]. This phase has been synthesized as low as $340\text{ }^\circ\text{C}$ and remains stable up to $711\text{ }^\circ\text{C}$ under its own vapour pressure.

Taking into account (i) all the characteristics of the third and fourth phases derived from the neutron thermodiffraction experiments, (ii) the experimental results on the analogue system Ag-Ge-S , and (iii) the composition diagram shown in figure 8, an assumption on the composition of the two phases can be proposed: Ag_2GeSe_3 and $\text{Ag}_{10}\text{Ge}_3\text{S}_{11}$. The first one has already appeared in the literature as a 'transient' phase in the ternary Ag-Ge-Se system and both of them have sulfide homologues. Ag_2GeSe_3 would appear first, and being an unstable compound it would decompose at higher temperature or after few hours to give $\text{Ag}_{10}\text{Ge}_3\text{S}_{11}$ and GeSe_2 according to the reaction



Such a scheme would be in agreement with the increase in intensity of the peaks related to GeSe_2 when the unstable

Ag_2GeSe_3 phase starts decomposing. The additional peaks found in the thermodiffraction pattern in addition to those related to the stable Ag_8GeSe_6 and GeSe_2 phases would be the signature of the new $\text{Ag}_{10}\text{Ge}_3\text{Se}_{11}$ phase.

Note that all our efforts to prepare pure Ag_2GeSe_3 and $\text{Ag}_{10}\text{Ge}_3\text{Se}_{11}$ phases failed.

5. Conclusions

The neutron thermodiffraction study, using either heating ramps or isotherm experiments, allowed us to get insight into the crystallization process of the three $\text{Ag}_x(\text{Ge}_{0.25}\text{Se}_{0.75})_{100-x}$ glasses ($x = 5, 15$ and 25). For all glasses the main products of crystallization were the two stable phases Ag_8GeSe_6 and GeSe_2 . However, the crystallization process of the Ag-rich glasses was more complex. An additional phase, i.e. Ag_2GeSe_3 , appeared at high temperature. Such a phase was unstable since it decomposed after a few hours of existence to give a new phase, $\text{Ag}_{10}\text{Ge}_3\text{Se}_{11}$, along with the stable GeSe_2 . While the unstable Ag_2GeSe_3 had already been reported in the literature even though controversies existed, $\text{Ag}_{10}\text{Ge}_3\text{Se}_{11}$ is reported for the first time.

Acknowledgments

The skilful technical assistance of Alain Daramsy (ILL, Grenoble, France) is gratefully acknowledged. Financial support from the CEA-LETI is gratefully acknowledged. The work was carried out in the framework of the Project ANR-05-BLAN-0058-01.

References

- [1] Piarristeguy A A, Mirandou M, Fontana M and Arcondo B 2000 *J. Non-Cryst. Solids* **273** 30
- [2] Dejus R J, Susman S, Volin K J, Montague D G and Price D L 1992 *J. Non-Cryst. Solids* **143** 162
- [3] Mitkova M, Wang Yu and Boolchand P 1999 *Phys. Rev. Lett.* **83** 3848
- [4] Kawasaki M, Kawamura J, Nakamura Y and Aniya M 1999 *J. Non-Cryst. Solids* **123** 259
- [5] Ureña M A, Fontana M, Arcondo B and Clavaguera-Mora M T 2003 *J. Non-Cryst. Solids* **320** 151
- [6] Ureña M A, Piarristeguy A A, Fontana M and Arcondo B 2005 *Solid State Ion.* **176** 505
- [7] Wang Y, Mitkova M, Georgiev D G, Mamedov S and Boolchand P 2003 *J. Phys.: Condens. Matter* **15** S1573
- [8] Gutenev M, Tabolin A and Rykova A 1991 *Fiz. Khim. Stakla* **17** 36
- [9] Pradel A and Ribes M 1992 *J. Solid State Chem.* **96** 247
- [10] Kolobov A V and Tanaka K 2001 *Handbook of Advanced Electronic and Photonic Materials and Devices* vol 5, ed H S Nalwa (New York: Academic) p 47
- [11] Kozicki M N, Mitkova M, Park M, Balakrishnan M and Gopalan C 2003 *Superlatt. Microstruct.* **34** 459
- [12] Piarristeguy A A, Ramonda M, Ureña M A, Pradel A and Ribes M 2007 *J. Non-Cryst. Solids* **353** 1261
- [13] Balan V, Piarristeguy A A, Ramonda M, Pradel A and Ribes M 2006 *J. Optoelectron. Adv. Mater.* **8** 2112
- [14] Cuello G J, Piarristeguy A A, Fernández-Martínez A, Fontana M and Pradel A 2007 *J. Non-Cryst. Solids* **353** 729
- [15] Piarristeguy A A *et al* 2008 in preparation
- [16] Piarristeguy A A, Cuello G J, Arcondo B, Pradel A and Ribes M 2007 *J. Non-Cryst. Solids* **353** 1243
- [17] Rodríguez-Carvajal J 1993 *Physica B* **192** 55
- [18] Prince A 1988 *Ternary Alloys* ed G Petzow and G Effenberg (New York: VCH) p 195
- [19] Boucher F, Evain M and Brec R 1993 *J. Solid State Chem.* **107** 332
- [20] Ollitrault-Fichet R, Rivet J and Flahaut J 1985 *J. Less-Common Met.* **114** 273
- [21] Movsum-Zade A A, Salaeva Z Yu and Allazov M R 1987 *Zh. Neorg. Khim.* **32** 1705
- [22] Velázquez-Velázquez A, Belandría E, Fernández B J, Ávila Godoy R, Delgado G and Acosta-Najarro G D 2000 *Phys. Status Solidi* **220** 683
- [23] Mikolaichuk A G and Moroz V N 1987 *Zh. Neorg. Khim.* **32** 2312
- [24] Wang N 1980 *N. Jb. Miner. Abh.* **139** 139
- [25] Nagel A and Range K 1978 *Z. Naturf. b* **33** 1461